

A nodally bound-preserving discontinuous Galerkin method for the drift-diffusion equation

Gabriel R. Barrenechea^a, Tristan Pryer^b, Alex Trenam^{b,*}

^a*Department of Mathematics and Statistics, University of Strathclyde, 26 Richmond Street, Glasgow, G1 1XH, UK*

^b*Department of Mathematical Sciences, University of Bath, Claverton Down, Bath, BA2 7AY, UK*

Abstract

In this work, we introduce and analyse discontinuous Galerkin (dG) methods for the drift-diffusion model. We explore two dG formulations: a classical interior penalty approach and a nodally bound-preserving method. Whilst the interior penalty method demonstrates well-posedness and convergence, it fails to guarantee non-negativity of the solution. To address this deficit, which is often important to ensure in applications, we employ a positivity-preserving method based on a convex subset formulation, ensuring the non-negativity of the solution at the Lagrange nodes. We validate our findings by summarising extensive numerical experiments, highlighting the novelty and effectiveness of our approach in handling the complexities of charge carrier transport.

Keywords:

2010 MSC: 65M60,

2010 MSC: 65M22

1. Introduction

Charge carrier transport is a physical process concerned with the interaction of mobile charge carriers in the presence of an electric field. Modelling this process is of interest in many applications including battery electrolytes, fuel cells, ion membrane channels, plasma physics, semi-conductor devices, etc. (see e.g. [Jü09, wWZCX12] for details). The typical scale of applications means that molecular dynamics approaches are often computationally impractical, despite offering the most detailed physical description. Continuum models are a common alternative, and include the Poisson-Nernst-Planck (PNP) system, also known as the drift-diffusion equations (or Van Roosbroeck equations in semi-conductor literature).

In this work we introduce and analyse a new discontinuous Galerkin (dG) method for the drift-diffusion model:

$$\partial_t u = \operatorname{div}(\nabla u + u \nabla \psi), \quad (1)$$

where ψ is a prescribed electric potential and u the particle concentration. We are interested in this as a prototypical example of an electrolyte model that extends to the classical (normalised) two-species PNP equations

$$\begin{aligned} \partial_t \rho &= \operatorname{div}(\nabla \rho + \rho \nabla \psi) \\ \partial_t \nu &= \operatorname{div}(\nabla \nu - \nu \nabla \psi) \\ -\operatorname{div}(\varepsilon \nabla \psi) &= \rho - \nu + f, \end{aligned} \quad (2)$$

*Corresponding author

Email addresses: gabriel.barrenechea@strath.ac.uk (Gabriel R. Barrenechea), tmp38@bath.ac.uk (Tristan Pryer), amt83@bath.ac.uk (Alex Trenam)

where ρ and ν , respectively, represent positively and negatively charged particle concentrations, and the electric potential ψ is now a variable [Ner89, Pla90, DH23]. The electric permittivity is $\varepsilon > 0$, and $f \geq 0$ is the background fixed charge density.

The drift-diffusion equation (1) is an advection-diffusion equation, where the advection is the gradient of the electric potential. There is a rich body of literature concerning numerical methods (finite difference, finite volume, finite element, etc.) for advection-diffusion equations [Roo08, HV03]. In view of our application to concentrations (which must remain positive to make sense physically), we highlight the recent review of finite element methods respecting the discrete maximum principle for this problem [BJK24]. The presence of boundary and interior layers present a particular challenge due to the propensity of typical finite element solutions to display spurious oscillations around (pseudo-)discontinuities. In many cases these oscillations cause the solution to become negative.

Maintaining the positivity of concentration variables in the PNP system (2) is not only desirable for physical interpretations but is integral to the stability of the solution and the satisfaction of an associated energy decay [Gaj85]. Boundary layers, known physically as electrical double layers, can occur close to charged surfaces due to an exponential decay in electric potential [Bag05]. The associated large values of $\nabla\psi$ lead to locally convection-dominated flow, an effect which is only exacerbated with the addition of a Navier-Stokes-governed fluid velocity [CI19].

A piecewise linear continuous Galerkin approximation of (2) is shown in [PS09] to satisfy an M-matrix property, which ensures the satisfaction of a discrete maximum principle. With dG methods there is no such guarantee, even for an interior penalty discretisation of pure diffusion [BJK24]. For the steady-state drift-diffusion scheme discretised with conforming piecewise linear finite elements, in [BMP89] different monotone finite element methods were proposed, all of them sharing the aim of rewriting the popular Sharfetter-Gummel finite volume scheme in a finite element way. The analysis of the methods is carried out by rewriting the problem as a mixed formulation. Some other methods, such as the dG schemes of [LW17] and [LWYY22], make use of positivity-preserving limiters to deal with this problem. Other approaches involve making a judicious change of variables to guarantee the positivity of the concentrations. Examples include the logarithmic change of variables used in [MXL16, FX22] and the Slotboom transformation utilised in [Slo73, XCLZ13]. The cost of making such substitutions is the introduction of further non-linearities to the already-non-linear system. In this paper we consider dG methods, which are well-suited to advection-dominated regimes due to the additional stability they offer.

With the PNP system in mind, we examine in this paper two methods for solving (1). The first is a classical dG formulation of the problem, and the second is a method where positivity of the concentration is hard-coded into the finite element space. For the classical methodology we are able to show well-posedness and conduct a convergence analysis, however, the methodology does not satisfy a positivity preservation property. That is, there is no guarantee that the solution does not become negative within the domain.

The second method aims to rectify this. The main idea behind the positivity enforcement is to utilise the methodology from [BGPV24, ABP24], where we define a closed convex subset of the standard dG space. Using this we formulate the problem as a variational inequality at each timestep. This guarantees that the dG solution is positive at the Lagrange nodes. We show the problem is well-posed and examine some of the qualitative properties of the solution. In our numerical experiments we then show that the second method preserves nodal positivity in the context of the PNP system.

The remainder of this paper is structured as follows: in §2 we fix some basic notation and discuss the model problem its properties; a temporal semi-discretisation is studied in §3 to transform the parabolic problem into a sequence of elliptic problems; in §4 and §5 we then introduce a dG spatial discretisation and a nodally bound-preserving extension; §6 is devoted to demonstrating the properties possessed by these discretisations through numerical experiments; and finally, §7 contains some concluding remarks.

2. The drift-diffusion equation

Let $\Omega \subset \mathbb{R}^d$, $d \leq 3$ be a bounded, polytopal domain with boundary $\partial\Omega$. Throughout this work we denote the standard Lebesgue spaces by $L^p(\Omega)$, $1 \leq p \leq \infty$, $\omega \subset \mathbb{R}^d$, $d = 1, 2, 3$, with corresponding norms $\|\cdot\|_{L^p(\omega)}$.

The L^2 inner product over ω is denoted $\langle \cdot, \cdot \rangle_\omega$, where the subscript is omitted when $\omega = \Omega$. We introduce the Sobolev spaces [Eva10, RR04, c.f.]

$$W^{m,p}(\Omega) := \{w \in L^p(\Omega) : D^\alpha w \in L^p(\Omega), \text{ for } |\alpha| \leq m\}, \quad (3)$$

which are equipped with norms and semi-norms

$$\|w\|_{W^{m,p}(\Omega)}^2 := \sum_{|\alpha| \leq m} \|D^\alpha w\|_{L^p(\Omega)}^2 \quad \text{and} \quad |w|_{W^{m,p}(\Omega)}^2 = \sum_{|\alpha|=m} \|D^\alpha w\|_{L^p(\Omega)}^2, \quad (4)$$

respectively, where $\alpha = \{\alpha_1, \dots, \alpha_d\}$ is a multi-index, $|\alpha| = \sum_{i=1}^d \alpha_i$ and derivatives D^α are understood in a weak sense. We identify the Hilbertian Sobolev spaces and norms by the notation $H^m(\Omega) := W^{m,2}(\Omega)$, and a zero subscript (e.g. $H_0^1(\Omega)$) indicates vanishing trace on $\partial\Omega$.

We consider the drift-diffusion equation, an advection-diffusion problem where the advection is the gradient of a potential $\psi = \psi(\mathbf{x}, t)$. In the context of electrolytes, this potential can be understood physically as the global electric potential, and $\nabla\psi$ is the electric field. In this viewpoint the solution variable $u = u(\mathbf{x}, t)$ represents the density of some charged particles, with an initial concentration profile given by u_0 . For simplicity of presentation, we suppose homogeneous Dirichlet boundary condition on $\partial\Omega \times (0, T]$, however, our results extend in a straightforward fashion to more general Dirichlet conditions (see [ABP24, BGPV24]). We explore such numerical examples in Section 6. Therefore, we seek u satisfying

$$\begin{aligned} \partial_t u &= \operatorname{div}(\nabla u + u \nabla \psi) \text{ in } \Omega_T, \\ u &= 0 \text{ on } \partial\Omega \times (0, T], \\ u &= u_0 \text{ on } \Omega \times \{0\}. \end{aligned} \quad (5)$$

Introducing the bilinear forms

$$a(w, v) := \int_{\Omega} \nabla w \cdot \nabla v \, d\mathbf{x}, \quad (6)$$

$$b(w, v) := \int_{\Omega} (w \nabla \psi) \cdot \nabla v \, d\mathbf{x}, \quad (7)$$

the initial-boundary value problem (5) can be written weakly as follows. Given $\psi \in W^{2,\infty}(\Omega)$ and initial data $0 \leq u_0 \in L^\infty(\Omega)$, seek $u(t) \in H_0^1(\Omega)$, for almost every $t \in (0, T]$, such that

$$\langle \partial_t u, v \rangle + a(u, v) + b(u, v) = 0 \quad \forall v \in H_0^1(\Omega). \quad (8)$$

Standard existence and uniqueness results for advection-diffusion equations (see [Eva10, RR04, c.f.]) apply to establish the well-posedness of (8).

Lemma 2.1 (PDE well-posedness). *Let $\psi \in W^{2,\infty}(\Omega)$ and $0 \leq u_0 \in L^\infty(\Omega)$. If $\Delta\psi \leq 0$, then there exists a unique solution $u(t) \in L^2((0, T]; H_0^1(\Omega)) \cap H^1((0, T]; H^{-1}(\Omega))$ to the weak IBVP (8).*

The problem (8) satisfies a stability result and a parabolic maximum principle, which we now detail. The preservation of these properties at the discrete level is the focus of the following sections. We begin with a useful lemma.

Lemma 2.2 (Energy identity). *Let $w \in H_0^1(\Omega)$ and $\psi \in W^{2,\infty}(\Omega)$. Then*

$$a(w, w) + b(w, w) = \|\nabla w\|_{L^2(\Omega)}^2 - \frac{1}{2} \langle \Delta\psi, w^2 \rangle. \quad (9)$$

Proof. Using the definition of $b(\cdot, \cdot)$ and integrating by parts yields

$$b(w, w) = \langle w \nabla \psi, \nabla w \rangle \quad (10)$$

$$= - \langle \operatorname{div}(w \nabla \psi), w \rangle. \quad (11)$$

Using the product rule and rearranging we obtain

$$b(w, w) = -\frac{1}{2} \langle \Delta \psi, w^2 \rangle. \quad (12)$$

The result then follows from the definition of $a(\cdot, \cdot)$. \square

Lemma 2.3 (Stability). *For almost every $t \in (0, T]$, let $u(t) \in H_0^1(\Omega)$ solve (8), with $\psi \in W^{2,\infty}(\Omega)$ and $0 \leq u_0 \in L^\infty(\Omega)$. Then we have*

$$\frac{d}{dt} \left[\frac{1}{2} \|u\|_{L^2(\Omega)}^2 \right] = -\|\nabla u\|_{L^2(\Omega)}^2 + \frac{1}{2} \langle \Delta \psi, u^2 \rangle. \quad (13)$$

The right hand side of the above equality is non-positive if $\Delta \psi \leq 0$.

Proof. Choosing $v = u$ in equation (8), we have

$$\frac{d}{dt} \left[\frac{1}{2} \|u\|^2 \right] = \langle \partial_t u, u \rangle = -a(u, u) - b(u, u), \quad (14)$$

and applying Lemma 2.2 completes the proof. \square

Lemma 2.4 (Parabolic Maximum Principle [RR04, Theorem 4.26]). *Let $u \in C^1((0, T]; H_0^1(\Omega))$ be a solution of the initial-boundary value problem (5) with $\psi \in W^{2,\infty}(\Omega)$ and $0 \leq u_0 \in L^\infty(\Omega)$. Suppose $\Delta \psi \leq 0$ in Ω . Then, for almost every $t \in (0, T]$, the solution satisfies the maximum principle*

$$0 \leq \inf_{\Omega} u_0 \leq \inf_{\Omega} u(t) \leq \sup_{\Omega} u(t) \leq \sup_{\Omega} u_0. \quad (15)$$

Proof. The proof follows from the classical parabolic maximum principle applied to the drift-diffusion equation (5) under the assumption $\Delta \psi \leq 0$. \square

3. A temporal semi-discretisation

In this section we examine an implicit backward Euler discretisation of the problem (8) and some of the properties inherited by this discretisation. We semi-discretise in time, and hence the parabolic problem is transformed into a sequence of elliptic problems.

For $N \in \mathbb{N}$, we define the set of discrete time steps $\{t^0, \dots, t^N\}$, with $0 = t^0 < t^1 < \dots < t^N = T$ and denote the time step size by τ . A variable w at time step t^n is denoted $w^n := w(t^n)$. Our arguments work with variable τ , but for simplicity of presentation we keep it fixed.

With the above notations (5) can be presented as a sequence of elliptic problems. Let $u^0 := u_0 \in L^\infty(\Omega)$, with $u_0 \geq 0$, and $\psi \in W^{2,\infty}(\Omega)$. For $n = 1, 2, \dots, N$ find $u^n \in H_0^1(\Omega)$ such that

$$\mathcal{A}(u^n, v) := \langle u^n, v \rangle + \tau(a(u^n, v) + b(u^n, v)) = \langle u^{n-1}, v \rangle \quad \forall v \in H_0^1(\Omega). \quad (16)$$

We now show that if $\Delta \psi \leq 0$, i.e., under the same assumption as Lemma 2.1, then (16) is well-posed. In addition, there is a time step condition which, if satisfied, guarantees well-posedness for any $\psi \in W^{2,\infty}(\Omega)$. The proof is based on the following coercivity and boundedness results regarding $\mathcal{A}(\cdot, \cdot)$.

Lemma 3.1 (Semi-discrete coercivity). *Let $w \in H_0^1(\Omega)$ and $\psi \in W^{2,\infty}(\Omega)$. If $\Delta \psi \leq 0$, then*

$$\mathcal{A}(w, w) \geq \|w\|_{L^2(\Omega)}^2 + \tau \|\nabla w\|_{L^2(\Omega)}^2. \quad (17)$$

Alternatively, removing the assumption of $\Delta \psi$, suppose instead that

$$\tau < \frac{4}{C_{\text{Sob}}^2 \|\Delta \psi\|_{L^3(\Omega)}^2}. \quad (18)$$

where C_{Sob} is the constant associated with the Sobolev embedding $H_0^1(\Omega) \hookrightarrow L^6(\Omega)$, which holds for $d \leq 3$. Then

$$\mathcal{A}(w, w) \geq \frac{1}{2} \|w\|_{L^2(\Omega)}^2 + \frac{\tau}{2} \|\nabla w\|_{L^2(\Omega)}^2. \quad (19)$$

Proof. From the definition of $\mathcal{A}(\cdot, \cdot)$ and Lemma 2.2, we have

$$\mathcal{A}(w, w) = \|w\|_{L^2(\Omega)}^2 + \tau a(w, w) + \tau b(w, w) \quad (20)$$

$$= \|w\|_{L^2(\Omega)}^2 + \tau \|\nabla w\|_{L^2(\Omega)}^2 - \frac{\tau}{2} \langle \Delta \psi, w^2 \rangle. \quad (21)$$

If $\Delta \psi \leq 0$, then (17) follows. Otherwise, we invoke the Sobolev embedding $H_0^1(\Omega) \hookrightarrow L^6(\Omega)$, for $d \leq 3$, and use Hölder's inequality to see that

$$\frac{\tau}{2} \langle \Delta \psi, w^2 \rangle \leq \frac{\tau}{2} \|\Delta \psi\|_{L^3(\Omega)} \|w\|_{L^6(\Omega)} \|w\|_{L^2(\Omega)} \quad (22)$$

$$\leq C_{\text{Sob}} \frac{\tau}{2} \|\Delta \psi\|_{L^3(\Omega)} \|\nabla w\|_{L^2(\Omega)} \|w\|_{L^2(\Omega)}. \quad (23)$$

Young's inequality then gives

$$\frac{\tau}{2} \langle \Delta \psi, w^2 \rangle \leq C_{\text{Sob}}^2 \frac{\tau^2}{8} \|\Delta \psi\|_{L^3(\Omega)}^2 \|\nabla w\|_{L^2(\Omega)}^2 + \frac{1}{2} \|w\|_{L^2(\Omega)}^2, \quad (24)$$

and therefore

$$\mathcal{A}(w, w) \geq \frac{1}{2} \|w\|_{L^2(\Omega)}^2 + \tau \left(1 - C_{\text{Sob}}^2 \frac{\tau}{8} \|\Delta \psi\|_{L^3(\Omega)}^2\right) \|\nabla w\|_{L^2(\Omega)}^2. \quad (25)$$

The result in (19) is then a consequence of the time step restriction (18). \square

Lemma 3.2 (Boundedness of $\mathcal{A}(\cdot, \cdot)$). *Let $w, v \in H_0^1(\Omega)$ and $\psi \in W^{2,\infty}(\Omega)$. Then*

$$\mathcal{A}(w, v) \leq \left(1 + C_P \|\nabla \psi\|_{L^\infty(\Omega)}\right) \left(\|w\|_{L^2(\Omega)}^2 + \tau \|\nabla w\|_{L^2(\Omega)}^2\right)^{1/2} \left(\|v\|_{L^2(\Omega)}^2 + \tau \|\nabla v\|_{L^2(\Omega)}^2\right)^{1/2}, \quad (26)$$

where C_P is the Poincaré constant.

Proof. Applying the Hölder and Poincaré inequalities to the definition of $\mathcal{A}(\cdot, \cdot)$ gives

$$\mathcal{A}(w, v) = \langle w, v \rangle + \tau a(w, v) + \tau b(w, v) \quad (27)$$

$$\leq \|w\|_{L^2(\Omega)} \|v\|_{L^2(\Omega)} + \tau \left(1 + C_P \|\nabla \psi\|_{L^\infty(\Omega)}\right) \|\nabla w\|_{L^2(\Omega)} \|\nabla v\|_{L^2(\Omega)} \quad (28)$$

$$\leq \left(1 + C_P \|\nabla \psi\|_{L^\infty(\Omega)}\right) \left(\|w\|_{L^2(\Omega)} \|v\|_{L^2(\Omega)} + \tau \|\nabla w\|_{L^2(\Omega)} \|\nabla v\|_{L^2(\Omega)}\right). \quad (29)$$

and using the discrete Cauchy-Schwarz inequality then yields the result. \square

Combining Lemma 3.1 and Lemma 3.2, the Lax-Milgram Lemma then yields the following result:

Corollary 3.3 (Existence and uniqueness of semi-discrete solution). *Under the conditions of Lemma 3.1, for $n = 1, 2, \dots, N$, there exists a unique $u^n \in H_0^1(\Omega)$ solving (16).*

The temporal semi-discretisation (16) satisfies the following stability and maximum principle results, which are semi-discrete analogues of the ones presented in Lemmata 2.3 and 2.4, respectively.

Lemma 3.4 (Semi-discrete stability). *Let the conditions of Lemma 3.1 be satisfied, with $\Delta \psi \leq 0$, and let $u^n \in H_0^1(\Omega)$ solve (16), for $n = 1, 2, \dots, N$. Then*

$$\frac{1}{2} \|u^n\|_{L^2(\Omega)}^2 \leq \frac{1}{2} \|u^{n-1}\|_{L^2(\Omega)}^2 - \tau \|\nabla u^n\|_{L^2(\Omega)}^2. \quad (30)$$

Proof. From (16) and Lemma 3.1 we have

$$\|u^n\|_{L^2(\Omega)}^2 + \tau \|\nabla u^n\|_{L^2(\Omega)}^2 \leq \mathcal{A}(u^n, u^n) = \langle u^{n-1}, u^n \rangle, \quad (31)$$

and the result follows by application of the Cauchy-Schwarz and Young inequalities. \square

Lemma 3.5 (Maximum Principle for the Semi-Discrete Problem). *Suppose $\psi \in W^{2,\infty}(\Omega)$ and $\Delta\psi \leq 0$ in Ω . Let $\{u^n\}_{n=0}^N$ be the sequence of solutions to the semi-discrete problem (16) with initial condition $u^0 = u_0 \in L^\infty(\Omega)$, where $u_0 \geq 0$. Then the following maximum principle holds:*

$$0 \leq \inf_{\Omega} u^0 \leq \inf_{\Omega} u^n \leq \sup_{\Omega} u^n \leq \sup_{\Omega} u^0, \quad \text{for all } n = 1, 2, \dots, N. \quad (32)$$

Proof. We prove the non-negativity of u^n by induction on n . For the base case, $n = 0$, the initial condition $u^0 = u_0 \in L^\infty(\Omega)$ is given and, by assumption, $u_0 \geq 0$. Now, assume inductively that $u^{n-1} \geq 0$ for some $n \geq 1$. We want to show that $u^n \geq 0$.

Let us begin by defining the positive and negative parts of u^n by $(u^n)_+ := \max(u^n, 0)$ and $(u^n)_- := u^n - (u^n)_+$, respectively. Then the mutually-disjoint support of $(u^n)_+$ and $(u^n)_-$ implies that

$$\langle u^n, (u^n)_- \rangle = \langle (u^n)_+ + (u^n)_-, (u^n)_- \rangle = \|(u^n)_-\|_{L^2(\Omega)}^2. \quad (33)$$

Choosing $v = (u^n)_-$ in (16) then leads to

$$\|(u^n)_-\|_{L^2(\Omega)}^2 = \langle u^{n-1}, (u^n)_- \rangle - \tau (a(u^n, (u^n)_-) + b(u^n, (u^n)_-)). \quad (34)$$

It follows from the inductive hypothesis that

$$\langle u^{n-1}, (u^n)_- \rangle \leq 0, \quad (35)$$

and using again the mutually-disjoint support of $(u^n)_+$ and $(u^n)_-$ then gives

$$\|(u^n)_-\|_{L^2(\Omega)}^2 \leq -\tau (a((u^n)_-, (u^n)_-) + b((u^n)_-, (u^n)_-)). \quad (36)$$

If $\Delta\psi \leq 0$, then Lemma 2.2 implies that

$$\|(u^n)_-\|_{L^2(\Omega)}^2 = 0, \quad (37)$$

and so $(u^n)_- \equiv 0$. In other words $u^n \geq 0$. The upper bound can be shown in a similar fashion taking $v = (u^n - \|u^0\|_{L^\infty(\Omega)})_+$. \square

4. A discontinuous Galerkin method

Let \mathcal{T} be a regular subdivision of Ω into disjoint simplicial or box-type (quadrilateral/hexahedral) elements K . We assume that the subdivision \mathcal{T} is shape-regular, that $\Omega = \bigcup_{K \in \mathcal{T}} \bar{K}$ and that the elemental faces are straight planar segments; these will be, henceforth, referred to as *facets*. By \mathcal{E} we shall denote the union of all 2-dimensional facets associated with the subdivision \mathcal{T} not including the boundary.

For $0 \leq p \in \mathbb{N}_0$ and a $K \in \mathcal{T}$ we denote the set of polynomials of total degree at most p by $\mathbb{P}^p(K)$ which allows us to define the discontinuous Galerkin finite element space

$$\mathbb{V}_p := \{w_h \in L^2(\Omega) : w_h|_K \in \mathbb{P}^p(K) \quad \forall K \in \mathcal{T}, \text{ and with vanishing trace on } \partial\Omega\}. \quad (38)$$

We also often make use of the set of Lagrange nodes $\{\mathbf{x}_i\}_{i=1}^{\dim(\mathbb{V}_p)}$. Let $K_1, K_2 \in \mathcal{T}$, with K_1 upwind from K_2 , be two elements sharing a facet $e \in \mathcal{E}$. For a function $w : \Omega \rightarrow \mathbb{R}$ we define the jump and average operators over e by

$$[[w]]_e := w|_{K_1} \mathbf{n}_{K_1} + w|_{K_2} \mathbf{n}_{K_2}, \quad \llbracket w \rrbracket_e := w|_{K_1} - w|_{K_2}, \quad \{ \! \! \{ w \} \! \! \}_e := \frac{1}{2} (w|_{K_1} + w|_{K_2}), \quad (39)$$

respectively. We will usually omit the subscript e . Let $h_K := \text{diam}(K)$ and $h \in \mathbb{V}_0$ to be the piecewise constant meshsize function such that $h|_K = h_K$.

Now we define the discontinuous Galerkin method. Let $0 \leq u_0 \in L^\infty(\Omega)$, $\psi \in W^{2,\infty}(\Omega)$, and $\Pi_h : L^2(\Omega) \rightarrow \mathbb{V}_p$ be the L^2 projection. For $u_h^0 = \Pi_h(u_0)$ and each $n = 1, 2, \dots, N$, find $u_h^n \in \mathbb{V}_p$ such that

$$\mathcal{A}_h(u_h^n, v_h) := \langle u_h^n, v_h \rangle + \tau(a_h(u_h^n, v_h) + b_h(u_h^n, v_h)) = \langle u_h^{n-1}, v_h \rangle \quad \forall v_h \in \mathbb{V}_p, \quad (40)$$

where, for $w, v \in H^2(\mathcal{T})$ and $\sigma, \mu > 0$,

$$a_h(w, v) := \sum_{K \in \mathcal{T}} \left(\int_K \nabla w \cdot \nabla v \, d\mathbf{x} \right) - \int_{\mathcal{E}} \left(\llbracket w \rrbracket \cdot \{\!\{ \nabla v \}\!\} + \llbracket v \rrbracket \cdot \{\!\{ \nabla w \}\!\} - \frac{\sigma}{h} \llbracket w \rrbracket \cdot \llbracket v \rrbracket \right) ds \quad (41)$$

and

$$b_h(w, v) := \sum_{K \in \mathcal{T}} \left(\int_K w \nabla \psi \cdot \nabla v \, d\mathbf{x} \right) - \int_{\mathcal{E}} \left((\nabla \psi \cdot \mathbf{n}) \llbracket w \rrbracket \llbracket v \rrbracket - \frac{\mu}{2} |\nabla \psi \cdot \mathbf{n}| \llbracket w \rrbracket \llbracket v \rrbracket \right) ds. \quad (42)$$

The bilinear form $a_h(\cdot, \cdot)$ is the symmetric interior penalty (SIP) discretisation of the diffusive term, which is coercive, assuming σ is chosen large enough, on \mathbb{V}_p under the norm

$$\|w_h\|_{\text{sip}}^2 := \|\nabla_h w_h\|_{L^2(\Omega)}^2 + \frac{\sigma}{h} \|\llbracket w_h \rrbracket\|_{L^2(\mathcal{E})}^2, \quad (43)$$

where σ depends on the polynomial degree p and geometric features of the mesh [CGH14].

Lemma 4.1 (SIP coercivity, e.g. [DE12, Lemma 4.12], [CDGH17, Lemma 27]). *Let $w_h \in \mathbb{V}_p$. There exists $\hat{\sigma} > 0$ and $C_C^{\text{sip}} > 0$, such that if $\sigma \geq \hat{\sigma}$, then*

$$a_h(w_h, w_h) \geq C_C^{\text{sip}} \|w_h\|_{\text{sip}}^2. \quad (44)$$

The bilinear form $b_h(\cdot, \cdot)$ is an upwinding discretisation of the advective term, where the classical upwinding method is recovered when $\mu = 1$. A natural notion of error when considering the problem (40) is the energy norm defined by

$$\|w_h\|^2 := \|w_h\|_{L^2(\Omega)}^2 + \tau \|w_h\|_{\text{sip}}^2 + \frac{\tau\mu}{2} \left\| |\nabla \psi \cdot \mathbf{n}|^{1/2} \llbracket w_h \rrbracket \right\|_{L^2(\mathcal{E})}^2, \quad (45)$$

and the well-posedness of the discrete problem is a consequence of the following coercivity result for the bilinear form $\mathcal{A}_h(\cdot, \cdot)$, the proof of which follows the same lines as [DE12, Lemma 4.59].

Lemma 4.2 (Discrete coercivity). *Let $w_h \in \mathbb{V}_p$ and $\psi \in W^{2,\infty}(\Omega)$. With C_C^{sip} and C_{Sob}^K defined as in Lemma 4.1. If $\Delta\psi \leq 0$, then $\mathcal{A}_h(\cdot, \cdot)$ is coercive on \mathbb{V}_p , with*

$$\mathcal{A}_h(w_h, w_h) \geq C_C \|w_h\|^2, \quad \text{where } C_C := \min\left(1, C_C^{\text{sip}}\right). \quad (46)$$

Otherwise, if $\Delta\psi \not\leq 0$, then $\mathcal{A}_h(\cdot, \cdot)$ is coercive on \mathbb{V}_p provided $\tau < 2 \|\Delta\psi\|_{L^\infty(\Omega)}^{-1}$, we have

$$\mathcal{A}_h(w_h, w_h) \geq C_C \|w_h\|^2, \quad \text{where } C_C := \min\left(1 - \frac{\tau}{2} \|\Delta\psi\|_{L^\infty(\Omega)}, C_C^{\text{sip}}\right). \quad (47)$$

Corollary 4.3. *Let $u_0 \in L^2(\Omega)$, and let the assumptions of Lemma 4.2 be satisfied. Then there exists a unique $u_h^n \in \mathbb{V}_p$ solving (40), for each $n = 1, 2, \dots, N$.*

The discrete solution to (40) enjoys the satisfaction of the following stability result.

Lemma 4.4 (Discrete stability). *Let the conditions of Lemma 4.2 be satisfied. For $n = 1, 2, \dots, N$, let $u_h^n \in \mathbb{V}_p$ be the solution to (40), with $0 \leq u_0 \in L^\infty(\Omega)$. Then*

$$\begin{aligned} \frac{1}{2} \|u_h^n\|_{L^2(\Omega)}^2 &\leq \frac{1}{2} \|u_h^{n-1}\|_{L^2(\Omega)}^2 - C_C^{\text{sip}} \tau \|u_h^n\|_{\text{sip}}^2 - \frac{\tau\mu}{2} \left\| |\nabla \psi \cdot \mathbf{n}|^{1/2} \llbracket u_h^n \rrbracket \right\|_{L^2(\mathcal{E})}^2 \\ &\quad - \tau \sum_{K \in \mathcal{T}} \left(-\frac{1}{2} \int_K (u_h^n)^2 \Delta\psi \, d\mathbf{x} \right), \end{aligned} \quad (48)$$

which is monotonically decreasing if $\Delta\psi \leq 0$.

Proof. Integrating (42) by parts, for all $w_h \in \mathbb{V}_p$, we find that

$$b_h(w_h, w_h) = \sum_{K \in \mathcal{T}} \left(-\frac{1}{2} \int_K w_h^2 \Delta \psi \, d\mathbf{x} \right) + \frac{\mu}{2} \left\| |\nabla \psi \cdot \mathbf{n}|^{1/2} \llbracket w_h \rrbracket \right\|_{L^2(\mathcal{E})}^2. \quad (49)$$

Choosing $v_h = u_h$ in (40), we obtain

$$\mathcal{A}_h(u_h^n, u_h^n) = \langle u_h^{n-1}, u_h^n \rangle. \quad (50)$$

and then using Lemma 4.1, the Cauchy-Schwarz and Young inequalities, and (49) completes the proof. \square

Remark 4.5 (Non-conforming DMP). *In the conforming setting, at least with $\Delta \psi \leq 0$, we can use lumping to ensure the discrete problem forms an M-matrix at the algebraic level [Tho07] which guarantees a discrete maximum principle. In the non-conforming setting things are less clear due to the coupling between elements through the jump terms. It is unclear whether a DMP for a SIP discretisation can be proven for a simple diffusion equation, see [BJK24, §9.4] for a further discussion and references.*

4.6. A priori error analysis

In this section we show an a priori error bound in the energy norm for the discretisation (40). The error analysis is based on the following lemmata, see also [DGP20], where we make use of the stronger norm

$$\|w_h\|_*^2 := \|w_h\|^2 + \tau \left\| |\nabla \psi \cdot \mathbf{n}|^{1/2} \llbracket w_h \rrbracket \right\|_{L^2(\mathcal{E})}^2. \quad (51)$$

Lemma 4.7 (Boundedness of $\mathcal{A}_h(\cdot, \cdot)$). *Let $w_h, v_h \in H^2(\mathcal{T})$. There exists $C_B > 0$, such that*

$$\mathcal{A}_h(w_h, v_h) \leq C_B \|w_h\|_* \|v_h\|. \quad (52)$$

Lemma 4.8 (Consistency of $\mathcal{A}_h(\cdot, \cdot)$). *Let $u^n \in H^2(\Omega) \cap H_0^1(\Omega)$ solve (16), and let $u_h^n \in \mathbb{V}_p$ solve (40). Then*

$$\mathcal{A}_h(u^n - u_h^n, v_h) = \langle u^{n-1} - u_h^{n-1}, v_h \rangle \quad \forall v_h \in \mathbb{V}_p. \quad (53)$$

Proof. Let $A : H^2(\Omega) \rightarrow L^2(\Omega)$ be the operator associated with the bilinear form $\mathcal{A}(\cdot, \cdot)$. That is, for $w \in H^2(\Omega)$,

$$\langle Aw, v \rangle = \mathcal{A}(w, v) \quad \forall v \in L^2(\Omega). \quad (54)$$

The strong form of the temporal semi-discretisation (16) then reads: for $u^0 := u_0 \in L^\infty(\Omega)$, with $u_0 \geq 0$, and $n = 1, 2, \dots, N$, seek $u^n \in H^2(\Omega) \cap H_0^1(\Omega)$ such that

$$\langle Au^n, v \rangle = \langle u^{n-1}, v \rangle \quad \forall v \in L^2(\Omega). \quad (55)$$

Also, let $A_h : \mathbb{V}_p \rightarrow \mathbb{V}_p$ be the operator associated with the bilinear form $\mathcal{A}_h(\cdot, \cdot)$, i.e. for $w_h \in \mathbb{V}_p$,

$$\langle A_h w_h, v_h \rangle = \mathcal{A}_h(w_h, v_h) \quad \forall v_h \in \mathbb{V}_p. \quad (56)$$

As a result of the consistency of the discrete operator A_h , and using (55), we then have

$$\mathcal{A}_h(u^n, v_h) = \langle A_h u^n, v_h \rangle = \langle Au^n, v_h \rangle = \langle u^{n-1}, v_h \rangle \quad \forall v_h \in \mathbb{V}_p. \quad (57)$$

The result then follows by taking the difference of equations (57) and (40). \square

Lemma 4.9 (A Strang-type lemma). *For $n = 1, 2, \dots, N$, let $u^n \in H^2(\Omega) \cap H_0^1(\Omega)$ solve (16) and $u_h^n \in \mathbb{V}_p$ solve (40). Also, let C_C and C_B be defined as in Lemma 4.2 and Lemma 4.7, respectively. Under the assumptions of Lemma 4.2, we have*

$$\|u^n - u_h^n\| \leq \left(1 + \frac{C_B}{C_C} \right) \inf_{w_h \in \mathbb{V}_p} \|u^n - w_h\|_* + \frac{1}{C_C} \sup_{v_h \in \mathbb{V}_p} \frac{\langle u^{n-1} - u_h^{n-1}, v_h \rangle}{\|v_h\|}. \quad (58)$$

Proof. Let $w_h \in \mathbb{V}_p$. The triangle inequality gives

$$\|u^n - u_h^n\| \leq \|u^n - w_h\| + \|w_h - u_h^n\|, \quad (59)$$

and we now control the second term on the right-hand side. Using first Lemma 4.2 and then Lemma 4.8, it follows that

$$C_C \|w_h - u_h^n\|^2 \leq \mathcal{A}_h(w_h - u_h^n, w_h - u_h^n) \quad (60)$$

$$= \mathcal{A}_h(w_h - u^n, w_h - u_h^n) + \mathcal{A}_h(u^n - u_h^n, w_h - u_h^n) \quad (61)$$

$$= \mathcal{A}_h(w_h - u^n, w_h - u_h^n) + \langle u^{n-1} - u_h^{n-1}, w_h - u_h^n \rangle. \quad (62)$$

Lemma 4.7 then gives

$$C_C \|w_h - u_h^n\|^2 \leq \|w_h - u_h^n\| \left(C_B \|w_h - u^n\|_* + \frac{\langle u^{n-1} - u_h^{n-1}, w_h - u_h^n \rangle}{\|w_h - u_h^n\|} \right) \quad (63)$$

$$\leq \|w_h - u_h^n\| \left(C_B \|w_h - u^n\|_* + \sup_{v_h \in \mathbb{V}_p} \frac{\langle u^{n-1} - u_h^{n-1}, v_h \rangle}{\|v_h\|} \right), \quad (64)$$

and dividing by $C_C \|w_h - u_h^n\|$ results in

$$\|w_h - u_h^n\| \leq \frac{C_B}{C_C} \|w_h - u^n\|_* + \frac{1}{C_C} \sup_{v_h \in \mathbb{V}_p} \frac{\langle u^{n-1} - u_h^{n-1}, v_h \rangle}{\|v_h\|}. \quad (65)$$

Returning to (59), we thus have

$$\|u^n - u_h^n\| \leq \left(1 + \frac{C_B}{C_C}\right) \|u^n - w_h\|_* + \frac{1}{C_C} \sup_{v_h \in \mathbb{V}_p} \frac{\langle u^{n-1} - u_h^{n-1}, v_h \rangle}{\|v_h\|}, \quad (66)$$

and choosing $w_h \in \mathbb{V}_p$ to minimise $\|u^n - w_h\|_*$ completes the proof. \square

5. A bound-preserving method

As highlighted in Remark 4.5, there is no guarantee that the solution to the discontinuous Galerkin discretisation (40) respects a discrete maximum principle, like the semi-discrete problem was shown to in Lemma 3.5. In this section we adopt the approach first introduced for reaction-diffusion equations in [BGPV24], and extended to reaction-advection-diffusion equations in [ABP24], whereby we seek solutions that respect the bounds at, but not necessarily between, element nodes. Figure 1 demonstrates the concept for piecewise linear and piecewise quadratic polynomials in one dimension. We emphasise that for $p = 1$ the solution satisfies the bounds *globally*, and not just at the nodes.

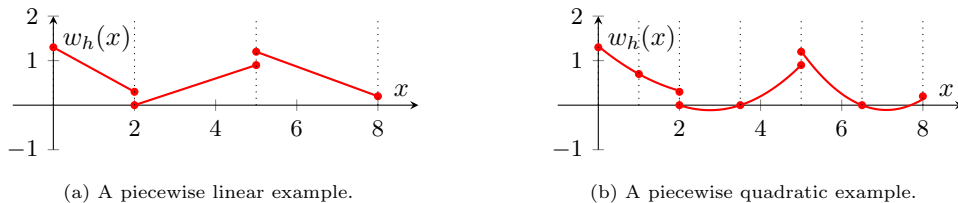


Figure 1: Examples of piecewise polynomial functions, on a non-uniform one-dimensional mesh, which are nodally non-negative. The dotted lines denote the locations of the Lagrange nodes of the elements. For piecewise linear functions the non-negativity is global, but for higher-order polynomials the function may go negative between the nodes.

Let us begin by defining the closed convex subset $\mathbb{V}_p^+ \subseteq \mathbb{V}_p$ by restricting finite element functions at the Lagrange nodes to be between zero and the supremal value of the initial condition:

$$\mathbb{V}_p^+ := \left\{ w_h \in \mathbb{V}_p : 0 \leq w_h(\mathbf{x}_i) \leq \|u_0\|_{L^\infty(\Omega)}, \text{ for } i = 1, \dots, \dim(\mathbb{V}_p) \right\}. \quad (67)$$

We then pose the following method, where we write $(u_h^n)^+ \in \mathbb{V}_p^+$ to distinguish the nodally bound-preserving (or *constrained*) solution from the *unconstrained* solution $u_h^n \in \mathbb{V}_p$ to (40).

Given $\psi \in W^{2,\infty}(\Omega)$ and initial data $0 \leq u_0 \in L^\infty(\Omega)$, so $u_h^0 = \Pi_h(u_0) \in \mathbb{V}_p$, seek $(u_h^n)^+ \in \mathbb{V}_p^+$, for $n = 1, 2, \dots, N$, such that

$$\mathcal{A}_h \left((u_h^n)^+, v_h - (u_h^n)^+ \right) \geq \left\langle (u_h^{n-1})^+, v_h - (u_h^n)^+ \right\rangle \quad \forall v_h \in \mathbb{V}_p^+. \quad (68)$$

Remark 5.1. A discrete approximation to the initial condition in \mathbb{V}_p^+ can be obtained using a bound-preserving operator $\Pi_h^+ : L^2(\Omega) \rightarrow \mathbb{V}_p^+$. If u_0 is smooth enough to admit point values we may use the Lagrange interpolant. If u_0 is less smooth then other constructions are available (see e.g. [AP24, CN00, Vee19]).

Lemma 5.2. Let $\psi \in W^{2,\infty}(\Omega)$ and $0 \leq u_0 \in L^\infty(\Omega)$. Suppose the conditions of Lemma 4.2 are satisfied. Then, for $n = 1, 2, \dots, N$, there exists a unique $(u_h^n)^+ \in \mathbb{V}_p^+$ that solves (68).

Proof. By Lemma 4.2, the bilinear form $\mathcal{A}_h(\cdot, \cdot)$ is coercive on \mathbb{V}_p under the stated assumptions. The result then follows by applying Stampacchia's Theorem ([KSS0, pg. 24, Theorem 2.1]). \square

By design, the solution of (68) is nodally bound-preserving. We now see that it also satisfies a discrete energy decay, which is similar to Lemma 4.4.

Lemma 5.3 (Discrete stability). Let the conditions of Lemma 4.2 be satisfied. For $n = 1, 2, \dots, N$, let $(u_h^n)^+ \in \mathbb{V}_p^+$ be the solution to (68), with $0 \leq u_0 \in L^\infty(\Omega)$. Then

$$\begin{aligned} \frac{1}{2} \left\| (u_h^n)^+ \right\|_{L^2(\Omega)}^2 &\leq \frac{1}{2} \left\| (u_h^{n-1})^+ \right\|_{L^2(\Omega)}^2 - \tau C_C^{\text{sip}} \left\| (u_h^n)^+ \right\|_{\text{sip}}^2 - \frac{\tau \mu}{2} \left\| |\nabla \psi \cdot \mathbf{n}|^{1/2} \left\| (u_h^n)^+ \right\| \right\|_{L^2(\mathcal{E})}^2 \\ &\quad - \tau \sum_{K \in \mathcal{T}} \left(-\frac{1}{2} \int_K \left((u_h^n)^+ \right)^2 \Delta \psi \, d\mathbf{x} \right), \end{aligned} \quad (69)$$

which is monotonically decreasing if $\Delta \psi \leq 0$.

Proof. Testing with $v_h = 0$ in (68), we obtain

$$\mathcal{A}_h \left((u_h^n)^+, (u_h^n)^+ \right) \leq \left\langle (u_h^{n-1})^+, (u_h^n)^+ \right\rangle, \quad (70)$$

and the result then follows the same argument as Lemma 4.4. \square

5.4. Higher-order time discretisations

Higher-order time discretisations can also be posed whilst retaining the structure preservation properties. For example, an unconstrained second-order Crank-Nicolson method would read as follows. Given $\psi \in W^{2,\infty}(\Omega)$ and $0 \leq u_0 \in L^\infty(\Omega)$, so $u_h^0 = \Pi_h(u_0) \in \mathbb{V}_p$, seek $u_h^n \in \mathbb{V}_p$, for $n = 1, 2, \dots, N$, such that

$$\langle u_h^n, v_h \rangle + \tau a_h \left(\frac{u_h^n + u_h^{n-1}}{2}, v_h \right) + \tau b_h \left(\frac{u_h^n + u_h^{n-1}}{2}, v_h \right) = \langle u_h^{n-1}, v_h \rangle \quad \forall v_h \in \mathbb{V}_p. \quad (71)$$

Then the following stability result, which is an analogue of Lemma 4.4 holds.

Lemma 5.5. *Let the conditions of Lemma 4.2 be satisfied, and let $u_h^n \in \mathbb{V}_p$ solve (71), for $n = 1, 2, \dots, N$. Then*

$$\begin{aligned} \frac{1}{2} \|u_h^n\|_{L^2(\Omega)}^2 &\leq \frac{1}{2} \|u_h^{n-1}\|_{L^2(\Omega)}^2 - \tau C_C^{\text{sip}} \left\| \frac{u_h^n + u_h^{n-1}}{2} \right\|_{\text{sip}}^2 - \frac{\tau\mu}{2} \left\| |\nabla\psi \cdot \mathbf{n}|^{1/2} \left\| \frac{u_h^n + u_h^{n-1}}{2} \right\| \right\|_{L^2(\mathcal{E})}^2 \\ &\quad - \tau \sum_{K \in \mathcal{T}} \left(-\frac{1}{2} \int_K \left(\frac{u_h^n + u_h^{n-1}}{2} \right)^2 \Delta\psi \, d\mathbf{x} \right), \end{aligned} \quad (72)$$

which is monotonically decreasing if $\Delta\psi \leq 0$.

Proof. Choosing $v_h = \frac{1}{2} (u_h^n + u_h^{n-1})$ in equation (71) gives

$$\frac{1}{2} \|u_h^n\|_{L^2(\Omega)}^2 = \frac{1}{2} \|u_h^{n-1}\|_{L^2(\Omega)}^2 - \tau a_h \left(\frac{u_h^n + u_h^{n-1}}{2}, \frac{u_h^n + u_h^{n-1}}{2} \right) - \tau b_h \left(\frac{u_h^n + u_h^{n-1}}{2}, \frac{u_h^n + u_h^{n-1}}{2} \right), \quad (73)$$

and the result then follows by Lemma 4.1 and (49). \square

A corresponding nodally bound-preserving Crank-Nicolson discretisation can be posed and the related analogue to Lemma 5.3 proceeds in a similar fashion to the backward Euler case.

5.6. A priori error analysis

The analysis for the nodally bound-preserving method follows from that of Section 4.6 without much modification. The main difference lies in the following lemma.

Lemma 5.7. *For $n = 1, 2, \dots, N$, let $u^n \in H^2(\Omega) \cap H_0^1(\Omega)$ solve (16) and $(u_h^n)^+ \in \mathbb{V}_p^+$ solve (68). Then*

$$\mathcal{A}_h \left(u^n - (u_h^n)^+, v_h - (u_h^n)^+ \right) \leq \left\langle u^{n-1} - (u_h^{n-1})^+, v_h - (u_h^n)^+ \right\rangle \quad \forall v_h \in \mathbb{V}_p^+. \quad (74)$$

Proof. From (57) it follows that

$$\mathcal{A}_h \left(u^n, v_h - (u_h^n)^+ \right) = \left\langle u^{n-1}, v_h - (u_h^n)^+ \right\rangle \quad \forall v_h \in \mathbb{V}_p^+, \quad (75)$$

and (68) implies that

$$-\mathcal{A}_h \left((u_h^n)^+, v_h - (u_h^n)^+ \right) \leq -\left\langle (u_h^{n-1})^+, v_h - (u_h^n)^+ \right\rangle \quad \forall v_h \in \mathbb{V}_p^+. \quad (76)$$

Combining these yields the result. \square

The proof of the following corollary now proceeds in the same way as that of Lemma 4.9, with Lemma 5.7 replacing Lemma 4.8 as appropriate.

Corollary 5.8. *For $n = 1, 2, \dots, N$, let $u^n \in H^2(\Omega) \cap H_0^1(\Omega)$ solve (16), let $(u_h^n)^+ \in \mathbb{V}_p^+$ solve (68), and let C_C and C_B be defined as in Lemma 4.2 and Lemma 4.7, respectively. Under the assumptions of Lemma 4.2, we have*

$$\left\| u^n - (u_h^n)^+ \right\| \leq \left(1 + \frac{C_B}{C_C} \right) \inf_{w_h \in \mathbb{V}_p^+} \|u^n - w_h\|_* + \frac{1}{C_C} \sup_{v_h \in \mathbb{V}_p} \frac{\left\langle u^{n-1} - (u_h^{n-1})^+, v_h \right\rangle}{\|v_h\|}. \quad (77)$$

6. Numerical Experiments

The nodally bound-preserving scheme (68) was implemented in the FEniCS (Legacy) software [LW10, LWH12], with the variational inequality treated at each time step via the following iterative approach [Kor76]. Let \mathbf{A} and \mathbf{L} be the assembled finite element stiffness matrix and load vector, respectively, let $\gamma > 0$, and let \mathcal{P} be the realisation of a projection of $u_h \in \mathbb{V}_p$ into \mathbb{V}_p^+ , which we define at the Lagrange nodes by

$$\mathcal{P}(u_h(\mathbf{x}_i)) := \min\left(\|u_0\|_{L^\infty(\Omega)}, \max(0, u_h(\mathbf{x}_i))\right), \quad \text{for } i = 1, 2, \dots, \dim(\mathbb{V}_p). \quad (78)$$

In Section 6.2 we observe the two-sided bound, however, in the other examples we remove the upper limit, since only positivity of the solutions can be shown. Taking \mathbf{u}^0 to be the solution vector obtained by solving (40), the iteration then proceeds as

$$\mathbf{v}^m = \mathcal{P}\left(\mathbf{u}^{m-1} - \gamma(\mathbf{A}\mathbf{u}^{m-1} - \mathbf{L})\right), \quad (79)$$

$$\mathbf{u}^m = \mathcal{P}\left(\mathbf{u}^{m-1} - \gamma(\mathbf{A}\mathbf{v}^m - \mathbf{L})\right), \quad (80)$$

and the process is terminated when $\|\mathbf{u}^m - \mathbf{u}^{m-1}\|_{\ell^2} < \text{tol} := 10^{-6}$.

The experiments are all carried out in two spatial dimensions on triangular meshes, and unless otherwise stated, we use piecewise linear elements, a direct linear solver, and take $\sigma = 10$, $\mu = 1$, and $\gamma = 10^{-5}$.

6.1. Convergence on a uniform mesh with a smooth solution

We begin by verifying the convergence properties of the discretisation (68) on a uniform triangular mesh with upper right diagonals of the domain $\Omega_T = (0, 1)^2 \times (0, 1/2]$, using polynomial degrees $p = 1, 2$. To obtain a manufactured solution we choose

$$u = \sin(\pi t) \sin(\pi x) \sin(\pi y), \quad (81)$$

$$\psi = \sin(\pi t) \cos(\pi x) \cos(\pi y), \quad (82)$$

and include an additional appropriate forcing term in (68). The initial condition is thus $u_0 = 0$. The error $\|u^N - (u_h^N)^+\|$ is examined on a sequence of successively finer meshes, with mesh size parameters chosen such that $h^{-1} = 4, 8, 16, 32, 64$, and we fix $\tau = h^{p+1}$. The results are depicted in Figure 2, and demonstrate $\mathcal{O}(h^{p+1})$ convergence. In this case the iteration given by (79) converged in a single step at each time step, meaning the solution to the dG scheme (40) satisfied the bounds at the nodes without the need for projection.

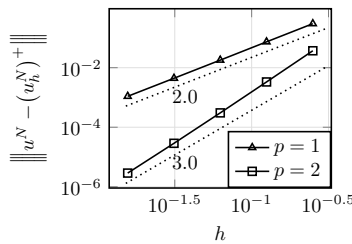


Figure 2: Convergence of the solution to (68) on a uniform mesh in the $\|\cdot\|$ -norm using piecewise polynomials of degree $p = 1, 2$. Convergence is observed at a rate of $\mathcal{O}(h^{p+1})$.

6.2. Structure preservation with discontinuous initial conditions

We begin to demonstrate the structure preservation of the method by investigating a problem setup with discontinuous initial conditions in a checkerboard-type pattern. Taking $\Omega_T = (0, 1)^2 \times (0, 0.03]$, we solve (68) with piecewise linear elements on a uniform triangular mesh with right-aligned diagonals, with mesh size

parameter $h = 0.01$ and time step size $\tau = 3 \times 10^{-4}$. At initial time the value of u_0 is either 0 or 1, as shown in Figure 3a, and we let $\psi = 100(x + y)$. We note that $\Delta\psi = 0$.

The evolution of the solution to (68) is shown through the snapshots in Figure 3, where the combination of the diffusive and advective behaviours can be seen. A boundary layer is formed towards the bottom left corner of the domain, and Figure 4a demonstrates that the the solution to (40) does not remain non-negative in the context of this problem, despite respecting the upper bound, as shown in Figure 4b. By design the nodally bound-preserving solution satisfies both constraints. We examine the L^2 -norm of the solution in Figure 4c, where monotonic decay is demonstrated for both solutions, in agreement with Lemma 4.4 and Lemma 5.3.

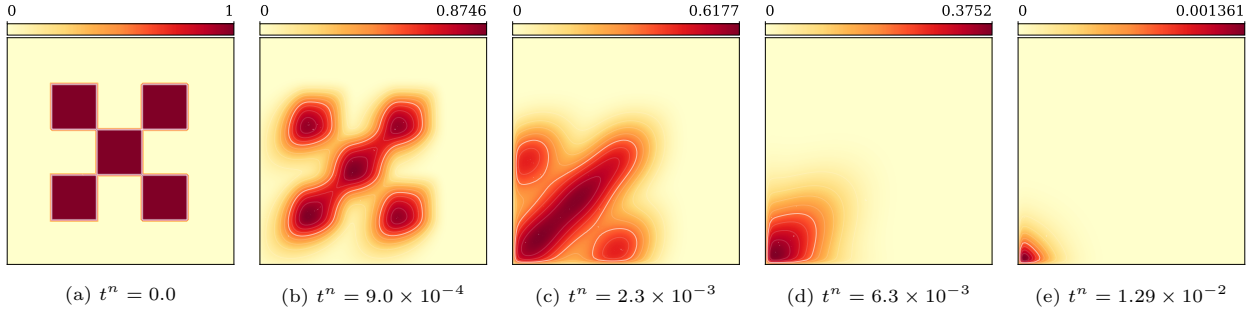


Figure 3: Snapshots of the solution to the example from Section 6.2.

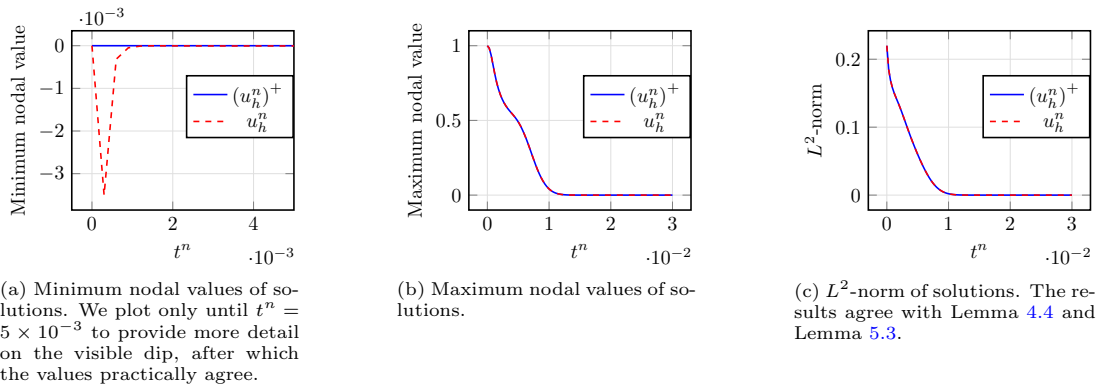


Figure 4: Plots comparing the nodally bound-preserving and unconstrained solutions for the example in Section 6.2.

6.3. Structure preservation with time-dependent boundary conditions

Next we consider a problem with non-homogeneous boundary conditions on a unit square spatial domain with a disc of radius 0.1 removed from the centre, and the temporal domain is the interval $(0, 1]$. We examine two different choices of ψ , given by $\psi_1 = 100 \sin(\pi(2x - 1/2))$ and $\psi_2 = -100 \sin(\pi(2x - 1/2))$, where we observe that $\Delta\psi_1 \leq 0$ and $\Delta\psi_2 \not\leq 0$ over the considered domain. Defining

$$g(t) := \frac{1}{2} + \frac{1}{2} \tanh\left(8\left(2t - \frac{1}{2}\right)\right), \quad (83)$$

we take the Dirichlet boundary conditions $u = 0$ on the boundary of the square and $u = g(t)$ on the boundary of the disc. The initial condition is taken as $u_0 = 0$. We solve the two problems using (68) with piecewise linear elements on a quasi-uniform Delaunay mesh of the domain that results in $\approx 68,000$ degrees of freedom. The time step size is fixed at $\tau = 0.01$, and for this problem we set $\sigma = 100$.

Figure 5a shows the solution at final time with ψ_1 , and 5b plots the minimum value of the solutions to both (40) and (68) over time, demonstrating the non-negativity of the latter in contrast to the former. We observe in Figure 5c the formation of boundary layers around the central disc for the problem involving ψ_2 . The resulting spurious oscillations are examined in greater detail in Figure 5d, where it can be seen that the solution to (40) becomes negative, whereas the nodally non-negative solution to (68) respects the bound. The oscillations also reduce in magnitude.

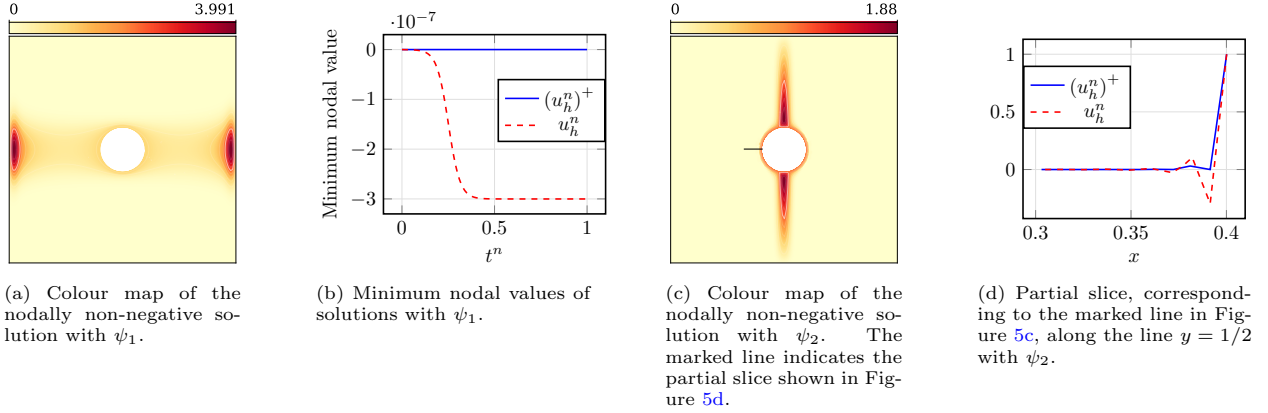


Figure 5: Snapshots at final time of the nodally non-negative solutions from the example in Section 6.3 and comparisons to the corresponding solutions to (40).

The energy change

$$E(w_h^n) := \left(\frac{1}{2} \|w_h^n\|_{L^2(\Omega)}^2 - \frac{1}{2} \|w_h^{n-1}\|_{L^2(\Omega)}^2 - \tau \int_{\partial\Omega} \left(w_h^n \nabla w_h^n \cdot \mathbf{n} + \frac{1}{2} (w_h^n)^2 (\nabla \psi \cdot \mathbf{n}) \right) ds \right)^{1/2}, \quad (84)$$

which arises from integrating by parts during the energy argument and accounts for the non-homogeneous boundary conditions, is plotted over time in Figure 6. We see the expected behaviour of monotonic energy decay when the condition $\Delta\psi \leq 0$ is satisfied, in agreement with Lemma 4.4 and Lemma 5.3.

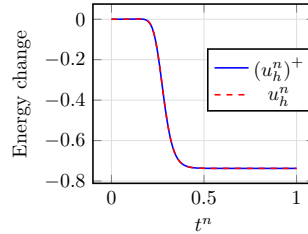


Figure 6: Evolution of the energy change (84) of the solution from Section 6.3 with $\psi = \psi_1$, where $\Delta\psi_1 \leq 0$. The results agree with Lemma 4.4 and Lemma 5.3.

6.4. An application to the coupled Poisson-Nernst-Planck system

In the final example we demonstrate the efficacy of our method as an approach to discretising the coupled Poisson-Nernst-Planck system (2) discussed in the introduction. In this case ψ is a variable at each time step, and so we introduce $\beta_h(\cdot; \cdot, \cdot)$, for all $\Psi \in H^1(\mathcal{T})$, $w, v \in H^2(\mathcal{T})$,

$$\beta_h(\Psi; w, v) := \sum_{K \in \mathcal{T}} \left(\int_K w \nabla \Psi \cdot \nabla v \, d\mathbf{x} \right) - \int_{\mathcal{E}} \left((\nabla \Psi \cdot \mathbf{n}) \{w\} \llbracket v \rrbracket - \frac{\mu}{2} |\nabla \Psi \cdot \mathbf{n}| \llbracket w \rrbracket \llbracket v \rrbracket \right) ds. \quad (85)$$

Notice that $\beta_h(\psi; w, v) = b_h(w, v)$. We then let

$$\mathfrak{A}_h(\Psi; w, v) := \langle w, v \rangle + \tau(a_h(w, v) + \beta_h(\Psi; w, v)), \quad (86)$$

the proposed numerical method is as follows. Given $\varepsilon > 0$ and $f, \rho_0, \nu_0 \in L^\infty(\Omega)$, so $(\rho_h^0)^+ = \Pi_h(\rho_0)$ and $(\nu_h^0)^+ = \Pi_h(\nu_0)$, for $n = 1, 2, \dots, N$, seek $((\rho_h^n)^+, (\nu_h^n)^+, \psi_h^n) \in \mathbb{V}_p^+ \times \mathbb{V}_p^+ \times \mathbb{V}_p$, such that

$$\mathfrak{A}_h(\psi_h^{n-1}; (\rho_h^n)^+, \phi_1 - (\rho_h^n)^+) \geq \langle (\rho_h^{n-1})^+, \phi_1 - (\rho_h^n)^+ \rangle \quad \forall \phi_1 \in \mathbb{V}_p^+, \quad (87)$$

$$\mathfrak{A}_h(\psi_h^{n-1}; (\nu_h^n)^+, \phi_2 - (\nu_h^n)^+) \geq \langle (\nu_h^{n-1})^+, \phi_2 - (\nu_h^n)^+ \rangle \quad \forall \phi_2 \in \mathbb{V}_p^+, \quad (88)$$

$$\varepsilon a_h(\psi_h^n, \Phi) = \langle (\rho_h^n)^+ - (\nu_h^n)^+ + f, \Phi \rangle \quad \forall \Phi \in \mathbb{V}_p. \quad (89)$$

By taking the value of ψ_h at the previous time step, equations (87) and (88) are instances of the nodally non-negative discretisation of the drift-diffusion equation given by (68). As a consequence the system can be decoupled by first solving (87) and (88), and then (89). At the initial time step only (89) need be solved.

We test the method (87)–(89) over the time interval $(0, 0.3]$ on a uniform criss-cross triangulation of the unit square with piecewise linear elements, resulting in 360,000 combined degrees of freedom for all variables. Fixing $\tau = 5 \times 10^{-3}$ and $\sigma = 100$, we take $\varepsilon = 3 \times 10^{-4}$, and

$$f(x) := \begin{cases} -1, & x < 1/2, \\ 1, & x \geq 1/2, \end{cases} \quad \rho_0 = \nu_0 := \frac{5}{2} \exp\left(-\left(8\left(x - \frac{1}{2}\right)\right)^2 - \left(8\left(y - \frac{1}{2}\right)\right)^2\right). \quad (90)$$

Snapshots of the solution are shown in Figure 7. A supplementary video is included in the online submission of this work for more detail. After initially diffusing from the Gaussian initial condition, $(\rho_h)^+$ and $(\nu_h)^+$ develop localised regions of high concentration which oscillate between the left and right halves of the domain, increasing in magnitude and decreasing in area until reaching a peak at $t^n = 0.05$. The solutions then decay to zero. In Figure 8 the minimum nodal values of the concentrations are compared against a version of (87)–(89) which does not preserve nodal non-negativity – that is, where (87) and (88) are instances of (40) rather than (68). The method which does not preserve nodal non-negativity experiences significant oscillations and negative values around $t^n = 0.06$. By design the nodally non-negative solution does not become negative.

7. Concluding remarks

The dG methods introduced and analysed in this work are shown to converge optimally in the energy norm, and the nodally bound-preserving method respects a discrete analogy of the maximum principle enjoyed by the drift-diffusion equation. Both discretisations also satisfy an energy dissipation law under the same assumptions on the data as the PDE. Although we focus on a backward Euler time discretisation, we also demonstrate structure preservation for higher-order time discretisations and quantify the impact the choice of time discretisation has on convergence rate. The presentation of the nodally bound-preserving method in a variational inequality framework simplifies the treatment of the analysis, and the implementation is achieved via a straightforward iterative projection method at each time step. We summarise with extensive numerical experiments, which demonstrate the just-described properties and the effectiveness of the methods. Finally, with a view towards future work, we consider an extension to the coupled Poisson-Nernst-Planck system, showing the robustness of the bound preservation in this case.

Funding sources

AT is supported by a scholarship from the EPSRC Centre for Doctoral Training in Advanced Automotive Propulsion Systems (AAPS), under the project EP/S023364/1. TP is grateful for partial support from the EPSRC grants EP/X030067/1, EP/W026899/1. Both TP and GRB are supported by the Leverhulme Trust Research Project Grant RPG-2021-238.

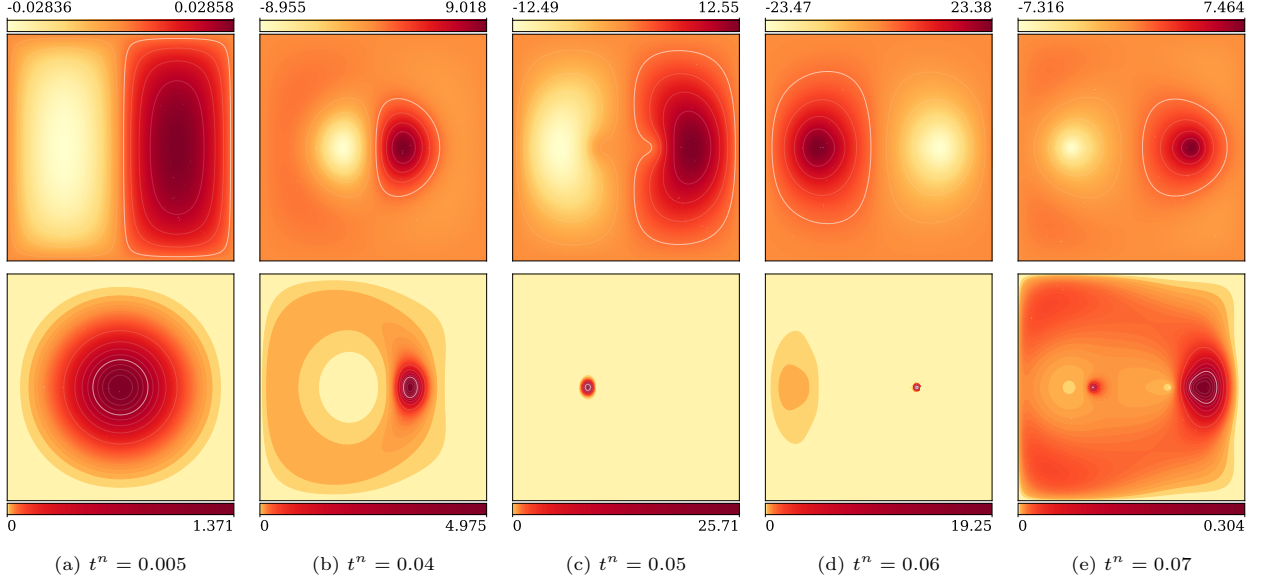


Figure 7: Snapshots of (top) ψ_h and (bottom) $(\rho_h)^+$ ($(\nu_h)^+$ is similar but reflected in the y -direction) from the numerical experiment in Section 6.4. We highlight that each subfigure has an individual colour bar and the plots for $(\rho_h)^+$ are plotted on a logarithmic scale.

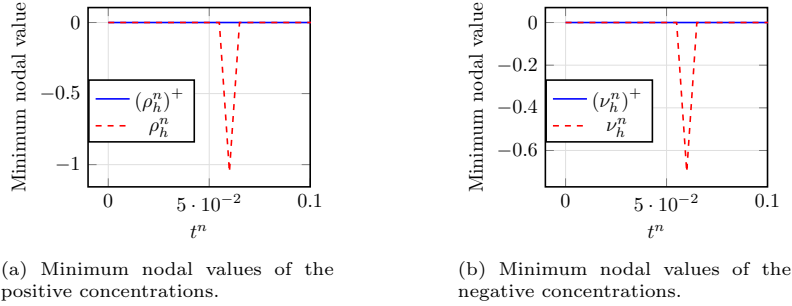


Figure 8: Evolution of the minimum nodal values of the solution to the example from Section 6.4. The values for the unconstrained solutions are also plotted for comparison.

References

- [ABP24] Abdolreza Amiri, Gabriel R. Barrenechea, and Tristan Pryer. A nodally bound-preserving finite element method for reaction–convection–diffusion equations. *Mathematical Models and Methods in Applied Sciences*, 34(08):1533–1565, 2024.
- [AP24] Ben S. Ashby and Tristan Pryer. Duality-based error control for the Signorini problem. *SIAM Journal on Numerical Analysis*, 62(4):1687–1712, 2024.
- [Bag05] V. S. Bagotsky. *Fundamentals of Electrochemistry*. Wiley, 2nd edition, 10 2005.
- [BGPV24] Gabriel R. Barrenechea, Emmanuil H. Georgoulis, Tristan Pryer, and Andreas Veerer. A nodally bound-preserving finite element method. *IMA Journal of Numerical Analysis*, 44(4):2198–2219, 2024.
- [BJK24] Gabriel R. Barrenechea, Volker John, and Petr Knobloch. Finite element methods respecting the discrete maximum principle for convection-diffusion equations. *SIAM Review*, 66(1):3–88, 2024.

- [BMP89] Franco Brezzi, Luisa Donatella Marini, and Paola Pietra. Two-dimensional exponential fitting and applications to drift-diffusion models. *SIAM J. Numer. Anal.*, 26(6):1342–1355, 1989.
- [CDGH17] Andrea Cangiani, Zhaonan Dong, Emmanuil H. Georgoulis, and Paul Houston. *hp-Version Discontinuous Galerkin Methods on Polygonal and Polyhedral Meshes*. Springer International Publishing, 1 edition, 2017.
- [CGH14] Andrea Cangiani, Emmanuil H. Georgoulis, and Paul Houston. *hp-version discontinuous Galerkin methods on polygonal and polyhedral meshes*. *Mathematical Models and Methods in Applied Sciences*, 24(10):2009–2041, 2014.
- [CI19] Peter Constantin and Mihaela Ignatova. On the Nernst-Planck-Navier-Stokes system. *Archive for Rational Mechanics and Analysis*, 232:1379–1428, 6 2019.
- [CN00] Zhiming Chen and Ricardo H. Nochetto. Residual type a posteriori error estimates for elliptic obstacle problems. *Numerische Mathematik*, 84:527–548, 2 2000.
- [DE12] Daniele Antonio Di Pietro and Alexandre Ern. *Mathematical aspects of discontinuous Galerkin methods*. Springer Berlin Heidelberg, 1 edition, 2012.
- [DGP20] Zhaonan Dong, Emmanuil H. Georgoulis, and Tristan Pryer. Recovered finite element methods on polygonal and polyhedral meshes. *ESAIM: Mathematical Modelling and Numerical Analysis*, 54(4):1309–1337, 2020.
- [DH23] Peter Debye and Erich Hückel. Zur theorie der elektrolyte. *Physikalische Zeitschrift*, 24:185–206, 1923.
- [Eva10] Lawrence C. Evans. *Partial Differential Equations*. American Mathematical Society, second edition, 2010.
- [FX22] Guosheng Fu and Zhiliang Xu. High-order space-time finite element methods for the Poisson-Nernst-Planck equations: Positivity and unconditional energy stability. *Computer Methods in Applied Mechanics and Engineering*, 395:115031, 5 2022.
- [Gaj85] H. Gajewski. On existence, uniqueness and asymptotic behavior of solutions of the basic equations for carrier transport in semiconductors. *ZAMM -Zeitschrift für Angewandte Mathematik und Mechanik*, 65:101–108, 1985.
- [HV03] W. Hundsdorfer and J. G. Verwer. *Numerical Solution of Time-Dependent Advection-Diffusion-Reaction Equations*. Springer-Verlag, 2003.
- [Jü09] Ansgar Jüngel. *Transport equations for semiconductors*, volume 773. Springer Berlin Heidelberg, 1 edition, 2009.
- [Kor76] G. M. Korpelevich. The extragradient method for finding saddle points and other problems. *Ekonomika i matematicheskie metody*, 12:747–756, 1976.
- [KS80] David Kinderlehrer and Guido Stampacchia. *An Introduction to Variational Inequalities and Their Applications*. Academic Press Inc., 1980.
- [LW10] Anders Logg and Garth N. Wells. DOLFIN: automated finite element computing. *ACM Transactions on Mathematical Software*, 37:1–28, 4 2010.
- [LW17] Hailiang Liu and Zhongming Wang. A free energy satisfying discontinuous Galerkin method for one-dimensional Poisson-Nernst-Planck systems. *Journal of Computational Physics*, 328:413–437, 10 2017.

- [LWH12] Anders Logg, Garth N. Wells, and J. Hake. *DOLFIN: a C++/Python finite element library*, volume 84. Springer Berlin Heidelberg, 2012.
- [LWYY22] Hailiang Liu, Zhongming Wang, Peimeng Yin, and Hui Yu. Positivity-preserving third order DG schemes for Poisson-Nernst-Planck equations. *Journal of Computational Physics*, 452:110777, 3 2022.
- [MXL16] Maximilian S. Metti, Jinchao Xu, and Chun Liu. Energetically stable discretizations for charge transport and electrokinetic models. *Journal of Computational Physics*, 306:1–18, 2 2016.
- [Ner89] Walther Nernst. Die elektromotorische wirksamkeit der jonen. *Zeitschrift für Physikalische Chemie*, 4U:129–181, 7 1889.
- [Pla90] Max Planck. Ueber die erregung von electricität und wärme in electrolyten. *Annalen der Physik und Chemie*, 275:161–186, 1890.
- [PS09] Andreas Prohl and Markus Schmuck. Convergent discretizations for the Nernst-Planck-Poisson system. *Numerische Mathematik*, 111:591–630, 2009.
- [Roo08] Hans-Görg Roos. *Robust numerical methods for singularly perturbed differential equations*. Springer, 2008.
- [RR04] Michael Renardy and Robert C. Rogers. *An Introduction to Partial Differential Equations*. Springer New York, 2 edition, 2004.
- [Slo73] J.W. Slotboom. Computer-aided two-dimensional analysis of bipolar transistors. *IEEE Transactions on Electron Devices*, 20(8):669–679, 1973.
- [Tho07] Vidar Thomée. *Galerkin finite element methods for parabolic problems*, volume 25. Springer Science & Business Media, 2007.
- [Vee19] Andreas Veese. Positivity preserving gradient approximation with linear finite elements. *Computational Methods in Applied Mathematics*, 19:295–310, 4 2019.
- [wWZCX12] Guo wei Wei, Qiong Zheng, Zhan Chen, and Kelin Xia. Variational multiscale models for charge transport. *SIAM Review*, 54:699–754, 1 2012.
- [XCLZ13] Yan Xie, Jie Cheng, Benzhuo Lu, and Linbo Zhang. Parallel adaptive finite element algorithms for solving the coupled electro-diffusion equations. *Computational and Mathematical Biophysics*, 1:90–108, 4 2013.